Theoretical Chemistry Accounts (2023) 142:93
https://doi.org/10.1007/s00214-023-03042-4

RESEARCH

Reactivity of alloxydim herbicide: force and reaction electronic flux profiles

Juan J. Villaverde[1] · Pilar Sandín-España[1] · José L. Alonso-Prados[1] · Manuel Alcamí[2,3,4] · Al Mokhtar Lamsabhi[2,3]

Received: 18 July 2023 / Accepted: 23 August 2023 / Published online: 15 September 2023

Abstract

The reaction force profile and the electronic reaction flux concepts were explored for the herbicide alloxydim and some of its derivatives at B3LYP/6-311G(d,p) level of theory. The exploration was achieved by rotating the oxime bond which is the most reactive region of the molecule. The main objective is to understand how the rotation of this bond influences the properties of the molecule and induces an electronic reorganization. The results show that the rotation of the dihedral angle triggers alloxydim to go through three transition states. The first step of the transformation begins by the rupture of the hydrogen bond and is characterized by a pronounced structural reorganization. In the last step of the process the electronic reorganization is more important.

Keywords Pesticides · Reaction force profile · Reaction electronic flux · Conceptual DFT

1 Introduction

The European Union (EU) has one of the most developed pesticide legislations. Since the adoption of the Council Directive 91/414/EEC, which was later replaced by the current Regulation (EC) No. 1107/2009 [1], any pesticide must past a rigorous assessment process that proves that its agronomic uses do not pose any risk for human and animal health and the environment before marketed in any Member State of the EU. Commission Regulation (EU) No 283/2013 [2] and 284/2013 [3] set out the data requirements for active substances and plant protection products, respectively, include a large number of experimental studies of different areas (identity, physical and chemical properties, methods of analysis, efficacy, toxicology, residues, environmental fate and behaviour and ecotoxicology). New approaches methodologies, such as quantitative structure–activity relationship (QSAR) and computational analytical methods are being considered by the European Food Safety Authority (EFSA) as an alternative to substitute vertebrate studies and other type of studies that nowadays are required, without prejudice the safety and the robustness of the risk assessment [4]. Provisions in Regulation (EC) No. 1107/2009 states that risk assessment of active substances and plant protection products shall be based on current scientific and technical knowledge, an alternative approach could take advantage of computational chemistry to accelerate the process [5].

To understand the reactivity of pesticides is key to predict their eco-toxicity and their environmental behaviour. Therefore, the study of these issues by ab initio or Density Functional Theory (DFT) methods might be an easy and costless task. Recently, we started different studies on the herbicide alloxydim (see Scheme 1) [6, 7]. From the theoretical point of view we have explored the stability of different isomers and conformers [8] and all possible degradation products (DPs) obtained after dissociation of the oxime fragment [9] as it is thought that the toxicity of this compound is linked to its ability to detach this group.

The mechanism of oxime intoxication is thought to lie in its interaction with nerve agents [10]. One key aspect that seems to determine its toxicity as poisoning or as a drug is the spatial orientation of the oxime group. Also, the side

✉ Manuel Alcamí
manuel.alcami@uam.es

1 Plant Protection Products Unit/Plant Protection Department, INIA-CSIC, Crta. La Coruña, Km. 7.5, 28040 Madrid, Spain

2 Departamento de Química, Facultad de Ciencias, Módulo 13, Universidad Autónoma de Madrid, 28049 Madrid, Spain

3 Institute for Advanced Research in Chemical Sciences (IAdChem), Universidad Autónoma de Madrid, 28049 Madrid, Spain

4 Instituto Madrileño de Estudios Avanzados en Nanociencias (IMDEA-Nanociencia), 28049 Madrid, Spain

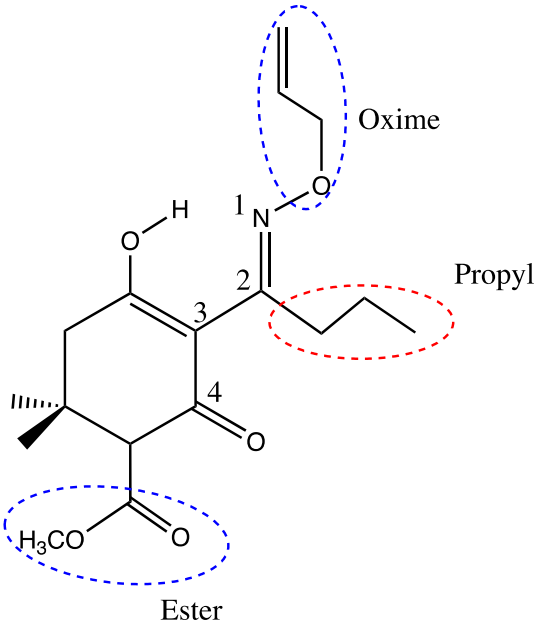

Scheme 1 Chemical structure of alloxydim herbicide. The surrounded areas indicate the functional groups that have a relevant role to determine the properties of the molecule

chain substituents at position 2 (see Scheme 1) in alloxydim derivatives show great influence in the herbicidal activity and therefore in its toxicity [7]. Substituents other than *n*-Pr, i.e. H and Ph, did not seem to have an important effect in the activity and toxicity.

The effect of rotation of chemical groups has been also studied in related systems as benzidine derivatives [11, 12] where relative low energy rotational barriers and therefore rotational freedom has been related with their capacity to freely interact with various components in biological media and is thus with their toxicity.

In the present study we aim to study how different properties change with the rotation of the oxime group (dihedral angle $N_1C_2C_3C_4$ in Scheme I), but avoiding the rupture of the oxime bond. Our main objective is to follow up the electronic and the structure variations with this dihedral angle. To get more insights on this perturbation we decided also to analyse the effect of the propyl group substitution by hydrogen, phenyl and chlorine group.

2 The theoretical framework

The intrinsic chemical change following a variation of one of the internal coordinates of a chemical entity can be understood in terms of geometrical changes and the reordering of the electron densities involved in the process [11]. Therefore, identifying structural and electronic changes taking place along the coordinate variation produces valuable information on the molecule transformation and can be analysed by the reaction force concept [13]. In fact, following the energy variation along the dihedral angle evolution could shed light on the different saddle points that encompass the reactivity of the systems under study. Starting from the structure with the lowest energy value associated to a given dihedral angle we can construct the energy profile, ($E(\theta)$), and connect different conformers through the corresponding transition states. The reaction force is defined as the derivative of $E(\theta)$ with respect to angle variation θ by the expression [14],

$$F(\theta) = -\frac{dE(\theta)}{d\theta} \tag{1}$$

For any elementary step of a chemical change, the reaction force is characterized by a minimum and a maximum located at ξ_1 and ξ_2 which delimitate three regions along the coordinate: the first one associated with the reactants ($\theta_R \le \theta \le \theta_1$) in which the reactants are prepared for the reaction mainly through structural reordering. The second one ($\theta_1 \le \theta \le \theta_2$) is the transition state region, corresponds to the region where most electronic changes due to bond formation and breaking take place. Finally, the third region, ($\theta_2 \le \theta \le \theta_P$), is associated with structural relaxation to reach the products of the reaction [15]. This well delimited reaction regions help to locate all the chemical events that take place in a reaction coordinate, thus giving a detailed picture of the system transformation. The activation energy and the energy necessary to attain the minima can also be obtained through the analysis of reaction force profile in the following decomposition in terms of reaction works.

$$\Delta E^{\neq} = W_1 + W_2 \tag{2}$$

where,

$$W_1 = -\int_{\theta_R}^{\theta_1} F(\theta)d\theta \text{ and } W_2 = -\int_{\theta_1}^{\theta_{TS}} F(\theta)d\theta \tag{3}$$

W_1 stands for the structural reorganizations to get the transition state from the reactant while W_2 encompasses the major electronic variations in the transition state region. θ_R and θ_{TS} delimit the activation region of the transition state. θ_1 is the coordinate where the reaction force attains its minimum inside this region.

To deeply understand the changes along the dihedral variation the conceptual DFT has been checked [16, 17]. This theory derives from DFT and offers an extended range of theoretical tools that can allow to study and understand the electronic changes which are directly associated to physicochemical properties of molecular systems. The electronic chemical potential, μ, for a system of N

electrons indicates the escaping tendency of electrons from sites of high chemical potential to low chemical potential and associated to the negative of electronegativity, χ [18]. It is defined as the derivative of the total energy with respect to N when the external potential, $v(r)$, remains constant.

$$\mu(r) = \left(\frac{\partial E(r)}{\partial N}\right)_{v(r)} = -\chi \tag{4}$$

The reaction electronic flux [19], $J(\theta)$, associated to a chemical transformation can be defined using Eq. 5:

$$J(\theta) = -\frac{d\mu(\theta)}{d\theta} \tag{5}$$

The interpretation of the reaction electronic flux results from the analogy with classical thermodynamics. Positive values of $J(\theta)$ should be associated to spontaneous rearrangements of the electron density driven by bond strengthening or forming processes; negative values of $J(\theta)$ are indicating nonspontaneous rearrangements of the electron density that are mainly driven by bond weakening or breaking processes [16].

3 Computational details

The optimization of the stationary points of structures under study was achieved at B3LYP/6-311G(d,p) level of theory [20, 21]. The rotation of the concerned fragment has been followed by a relaxed scan at the same level of theory by means of Gaussian 16 series of programs [22]. The electronic population analysis was done by the quantum theory of atoms in molecule theory (QTAIM), by using the AIMAll program [23].

4 Results and discussions

Our purpose, as mentioned above, is to highlight the electronic changes in alloxydim most reactive site. To get deeper insight on the different effects we substitute the propyl group by different substituents. As can be shown in Scheme 2, propyl was replaced by hydrogen, aryl or chlorine. To follow up the electronic and the structural changes of these derivates along the dihedral variation we constructed the energy profile starting from the most stable structure. This means that the exploration of the energy variation begins at $\theta_{N1,C2,C3,C4} \approx -180°$ and finishes at $\theta_{N1,C2,C3,C4} \approx 220°$. The choice of this structure comes of our recent exploration of the different isomers of the alloxydim [8].

Figure 1 shows the energy profile of the four compounds under study. The first conspicuous conclusion from this

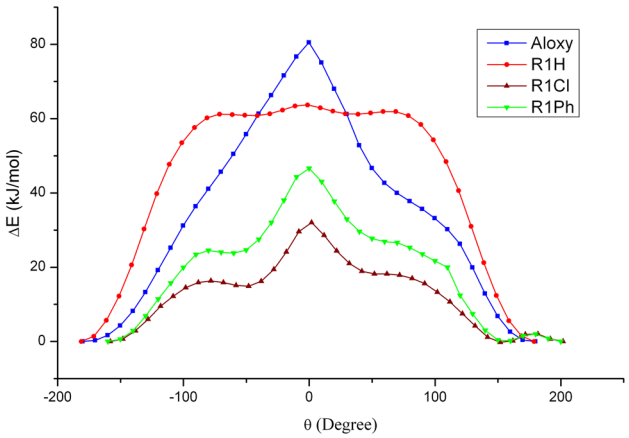

Fig. 1 Energy profile of alloxydim and its derivatives along the variation of the dihedral angle θ

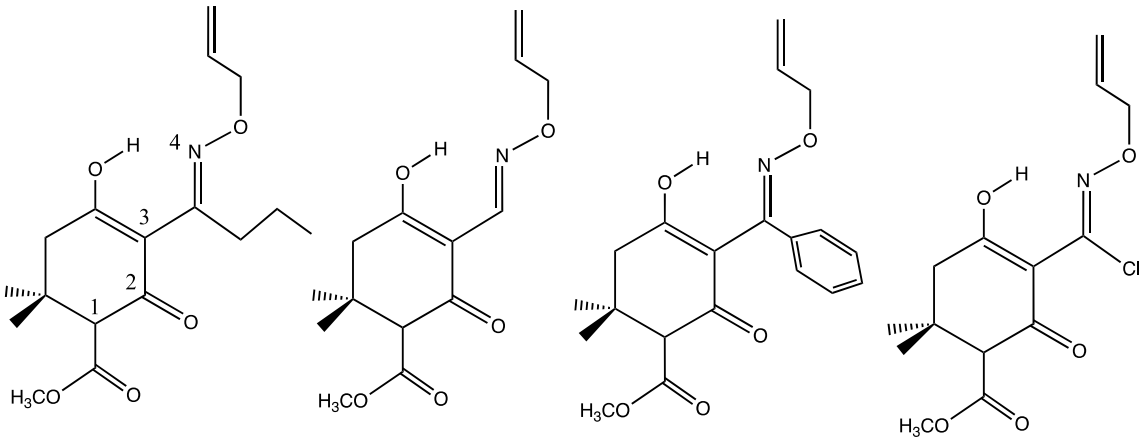

Scheme 2 Structures of the different derivatives of alloxydim under study

figure is that the rotation of the angle $\theta_{N1,C2,C3,C4}$ is energetically more demanding in alloxydim compared to the other species. Even with the electronic repulsion that can be presented by the aryl derivate alloxydim needs to overpass approximately more than 80 kJ/mol between the two minima while for the phenyl substitution this quantity does not exceed 54 kJ/mol. In the case of chlorine substitution, this value is about 33 kJ/mol. This is a simple image of the variation of the energy within the increase in the dihedral angle. However, if we explore the reaction force profile (see Fig. 2) we would be able to reach more valuable information. In fact, the reaction force profile as presented in Fig. 2 shows that the rotation process of the dihedral angle, θ, triggers alloxydim and its derivatives to go through three different maxima, called, TS1, TS2 and TS3. The minima between them are hidden due to the highest energy barriers obtained. Yet, the maxima have their origin on the middle point between two inflections of the reaction force curve which delimitate three regions of the compound transformation. Each one of these regions, as has been defined by Toro-labbé [10], can show the structural and the electronic reorganizations in each step of the systems under study. To quantify these transformations Toro-Labbé et al. proposed to calculate the works W_1 and W_2 and their participation in the activation energy, as defined above [19].

For alloxydim and its derivatives the rotation of the dihedral angle θ, shows that the system goes through three steps. The first one is associated to the rupture of the hydrogen bond (HB) in the most stable conformers and the weakening of the NO bond (see discussion below) and is shown the highest barrier energy along the process. Based on the works values $W1$ and $W2$ deduced from Fig. 2 and listed in Table 1, the highest activation energy is reported for R1 = H derivative. The structural rearrangement is about 53% of the activation energy, whereas the electronic reorganization is about 47%. The alloxydim on the other hand presents more structural than electronic reorganization with values about − 19.2 and 17.1 kJ/mol, respectively. This can be explained by the size of the isopropyl of alloxydim which needs more structural accommodation than the hydrogen as substituent. For the phenyl substituent, the structural and the electronic rearrangements to gain the first transition state, TS_1, are similar because probably of the π cloud of the aromatic substituent (see Table 1).

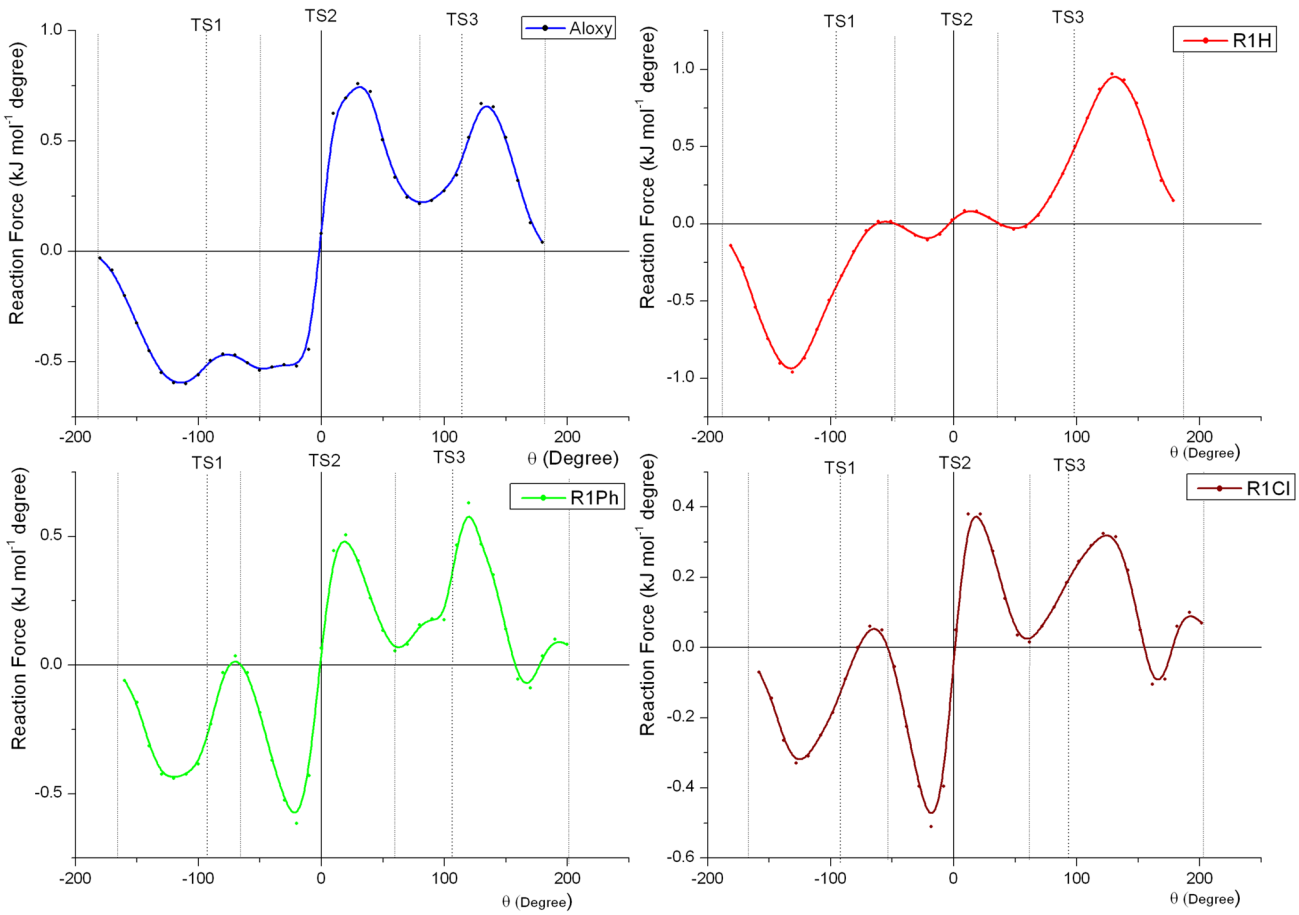

Fig. 2 The reaction force profile of alloxydim and its derivatives along the rotation

Table 1 Reaction works W_1 and W_2 performed by the system along the rotation of angle θ at each step of the process

	TS_1			TS_2			TS_3		
	W_1	W_2	$\Delta E^{\#}$	W_1	W_2	$\Delta E^{\#}$	W_1	W_2	$\Delta E^{\#}$
Alloxydim	19.2	17.1	36.3	15.7	6.7	22.3	0	12.2	12.2
R1 = H	30.3	26.9	57.2	1.4	1.1	2.5	0.5	7.95	7.5
R1 = Ph	11.4	11.4	22.8	14.0	7.1	21.1	0	8.5	8.5
R1 = Cl	6.1	9.6	15.7	9.1	6.2	15.3	0	2.8	2.8

$\Delta E^{\#}$ the energy barrier associated to each step. Values are in kJ/mol

Following the rotation of the dihedral angle the second step appears energetically less demanding than the first one. The highest barrier is observed for alloxydim and its phenyl derivate (R1 = Ph). In all the cases the structural reorganization is the dominant one. This is expected because this step represents a typical rotational transition state where the substituents moved by the angle should adapt their structure to fit with the new structural form of the molecule. It is worth noting that the lowest barrier is observed for R1 = H, about − 2.5 kJ/mol accordingly with the size of the substituent which does not require nor elevated structural nor electronic changes to overpass the transition state. In what concerns the last step of the energy profile, nearby TS_3, it is clear that structural movements are practically null in all the cases. The electronic rearrangement is the most dominant instead. This can be understood by the necessity of the system under study to attain again the HB arrangement which basically needs an electronic adaptation of the molecule.

The balance between the structural and the electronic changes along the angle variation in the energy profile can be viewed also by analysing the reaction electronic flux profile (Fig. 3). In fact, in the first step of the rotation of all

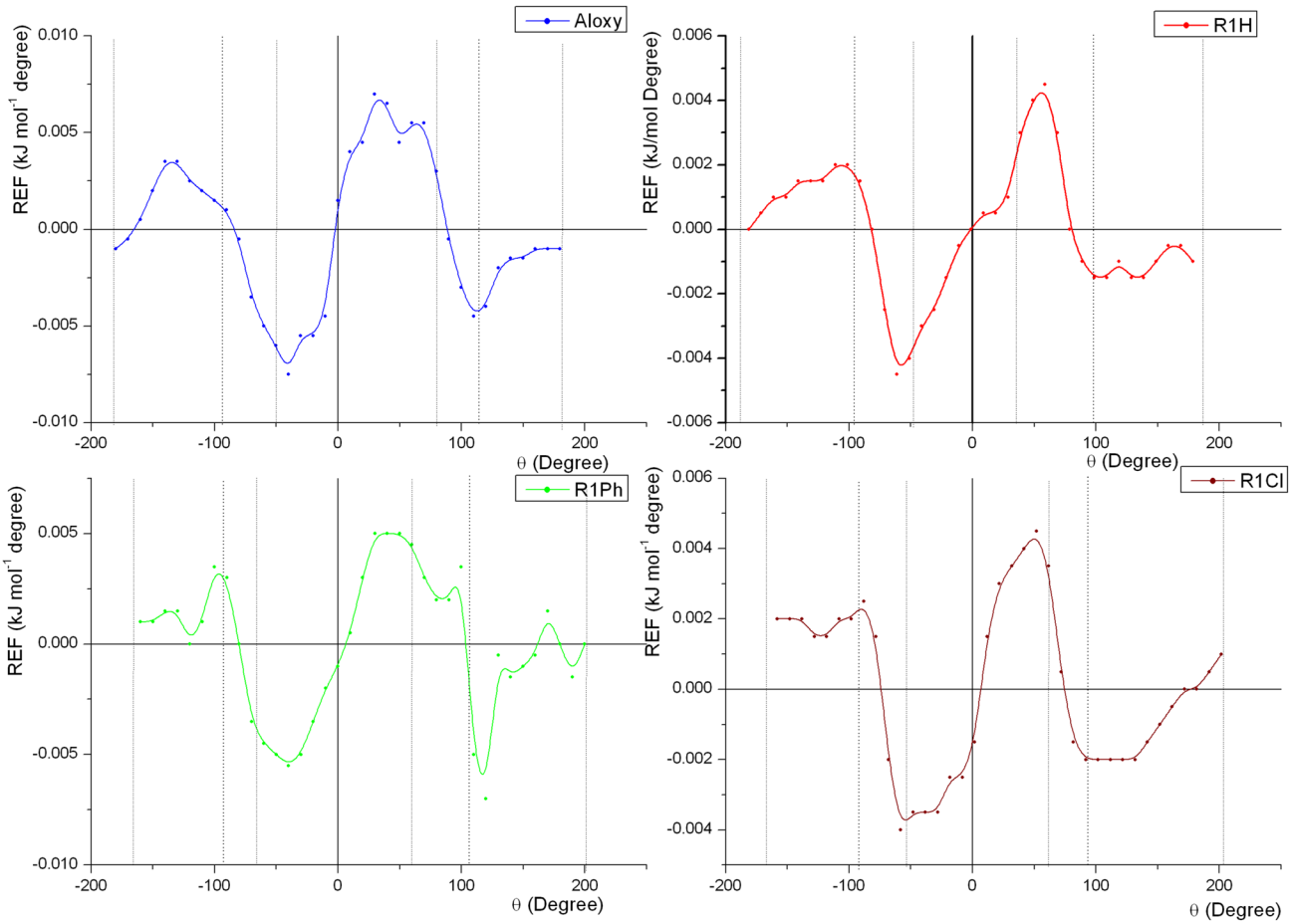

Fig. 3 Reaction electronic flux profile of the different substituents along the variation of the angle θ

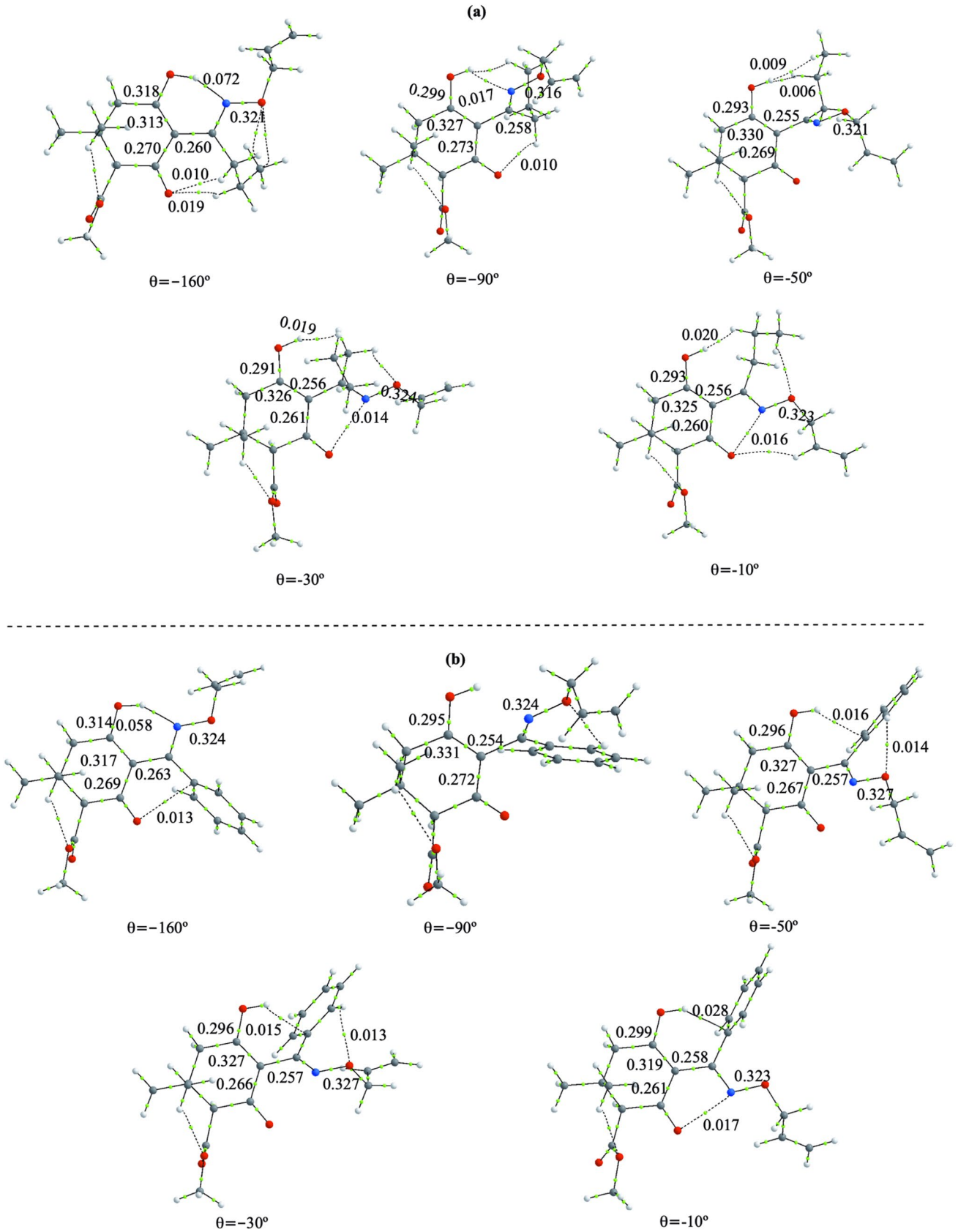

Fig. 4 The QTAIM analysis of some critical points along the θ variation in the case of (**a,** upper panel) alloxydim and (**b,** lower panel) its phenyl derivative (R1 = Ph). The values of densities at the BCP are in a.u

the systems under scrutiny we can observe a positive value of $J(\theta)$ which is an indication of a bond strengthening and spontaneous processes. Taking alloxydim as an example the evolution of the system in this step imply the rupture of the HB OH–N, between $\theta \approx -160°$ and $\theta \approx -90°$, with a reinforcement of the associated C–O bonds and the apparition of new weak HBs. This can be ratified by analysing different structures in some critical points of the energy profile by using the QTAIM population analysis. In Fig. 4a at the angle $\theta = -160$ we observe, for alloxydim, a HB provided by the hydroxyl group with an electronic density at the bond critical point (BCP) about 0.072 a.u. When moving to $\theta = -90$, the density at this BCP decreases to attain approximately 0.017 a.u. which is accompanied by the appearance of small H–H bonds which are basically provided by the CH groups. The oxime group along the rotation is affected by the structural and the electronic reorganization. In fact, in this first step while N–O bond along θ variation is slightly weakened (0.321–0.316 a.u.) the nearby bonds in 6-membered ring become reinforced (0.313–0.327 a.u.). This might be an indication that the rupture of the oxime group may occur during the first step of the conformational transformation.

The $J(\theta)$ profile presents negative values when the system overcomes the first transition state. This indicates that changes in the molecule go in the opposite direction than in the previous step. Form the QTAIM analysis given in Fig. 4a, N–O bond is slightly reinforced, and density goes back from 0.316 u.a. to 0.321 a.u. between $\theta \approx -90°$ and $\theta \approx -50°$, while some bonds of the six membered ring are weakened. After this point Fig. 4 shows very small variation of the density in the different BCP in agreement with the low values of W_1 reported in Table 1.

In the case of the phenyl counterpart from $\theta \approx -50°$, small HB interactions appear between the OH and the phenyl group as acceptor (see Fig. 4b) stabilizing the system along the rotation. This explain why the energy profile becomes lower and get flat around $\theta \approx -50°$, (see Fig. 1) and we obtain lower values of $\Delta E^{\#}$ specially for TS1 (see Table 1). The NO suffers smaller changes in the case of the phenyl derivative as seen in the BCP along the reaction coordinate (see Fig. 4b).

5 Conclusions

The intrinsic rotation of the dihedral angle θ of alloxydim and its derivatives shows that the system goes through three steps. The energy barrier in each step involves different interactions: breaking of HB, weakening of the NO, reinforcement of the six-membered ring and HB interaction with CH of isopropyl group in alloxydim or the aryl group in the phenyl derivative. The analysis of the force profile shows that the major structural reorganizations are done in the first step of the rotation process, where the N–O bond is weakened when moving the dihedral angle which might indicate that the oxime group could be dissociated along this stage. In this first step changes in the bond densities and energy barriers are larger for alloxydim and the H derivative which may be related with a higher toxicity of these two compounds.

Acknowledgements We acknowledge the financial support received by the project PID2019-110091GB-I00 and PDC2021-121203-I00 of the Ministerio de Ciencia, Innovación of Spain and by the project Y2020/EMT-6290 (PRIES-CM) of the Comunidad de Madrid. The authors would also like to thank the *Centro de Computación Científica* of the UAM (CCC-UAM) for the generous allocation of computer time and for their continued technical support.

Author contribution JJV and AML did most of the calculations; PS and JLA-P participated in the discussion and writing offering their point of view as experimentalists and experts in the determination of the environmental impact of pesticides. MA supervised the project and wrote the final version.

Funding Open Access funding provided thanks to the CRUE-CSIC agreement with Springer Nature. The work presented was funded by project PID2019-110091GB-I00 and PDC2021-121203-I00 of the Ministerio de Ciencia, Innovación of Spain and by the project Y2020/EMT-6290 (PRIES-CM) of the Comunidad de Madrid, Spain.

Data availability The datasets generated during and/or analysed during the current study are available from the corresponding author on reasonable request.

Declarations

Conflict of interest The authors have no competing interests as defined by Springer, or other interests that might be perceived to influence the results and/or discussion reported in this paper.

References

1. E. Union (2009) Regulation (EC) No 1107/2009, in Off J Eur Union L, 309:1
2. E. Union (2013) Regulation (EC) No 283/2013, in Off J Eur Union L, 93:1–84
3. E. Union (2013) Regulation (EC) No 284/2013, in Off J Eur Union L, 93:85–152
4. Cattaneo I, Astuto MC, Binaglia M, Devos Y, Dorne J-LCM, Ana FA, Fernandez DA, Garcia-Vello P, Kass GEN, Lanzoni A, Liem AKD, Panzarea M, Paraskevopulos K, Parra Morte JM, Tarazona JV, Terron A (2023) Implementing new approach methodologies

(NAMs) in food safety assessments: strategic objectives and actions taken by the European Food Safety Authority. Trends Food Sci Technol. https://doi.org/10.1016/j.tifs.2023.02.006
5. Villaverde JJ, López-Goti C, Alcamí M, Lamsabhi AM, Alonso-Prados JL, Sandín-España P (2017) Pest Manag Sci 73:2199
6. Sandín-España P, Sevilla-Morán B, Calvo L, Mateo-Miranda M, Alonso-Prados JL (2013) Microchem J 106:212
7. Villaverde JJ, Santín-Montanyá I, Sevilla-Morán B, Alonso-Prados JL, Sandín-España P (2018) Molecules 23:993
8. Villaverde JJ, Sandín-España P, Alonso-Prados JL, Lamsabhi AM, Alcamí M (2018) J Phys Chem A 122:3909
9. Villaverde JJ, Sandín-España P, Alonso-Prados JL, Lamsabhi AM, Alcamí M (2018) Comput Theor Chem 1143:9
10. Dhuguru J, Zviagin E, Skouta R (2022) Pharmaceuticals 15:66
11. Sarkar U, Roy DR, Chattaraj PK, Parthasarathi R, Padmanabhan J, Subramanian V (2005) J Chem Sci 117:599
12. Coburn JC, Soper PD, Auman BC (1995) Macromolecules 28:3253
13. Toro-Labbé A (1999) J Phys Chem A 103:4398
14. Martinez J, Toro-Labbé A (2009) J Math Chem 45:911
15. Herrera B, Toro-Labbé A (2001) Chem Phys Lett 344:193
16. Geerlings P (2022) Pharmaceuticals 15:1112
17. Geerlings P, De Proft F, Langenaeker W (2003) Chem Rev 103:1793
18. Parr RG, Yang W (1989) Density functional theory of atoms and molecules. Oxford University Press, New York
19. Echegaray E, Toro-Labbé A (2008) J Phys Chem A 112:11801
20. Becke AD (1993) J Chem Phys 98:5648
21. Lee CT, Yang WT, Parr RG (1988) Phys Rev B 37:785
22. Frisch MJ, Trucks GW, Schlegel HB, Scuseria GE, Frisch H, Trucks MJ, Schlegel GW, Scuseria HB, Robb GE, Cheeseman MA, Scalmani JR, Barone G, Mennucci V, Petersson B, Nakatsuji GA, Caricato H, Li M, Hratchian X, Izmaylov HP, Bloino AF, Zheng J, Sonnenberg G, Hada JL, Ehara M, Toyota M, Fukuda K, Hasegawa R, Ishida J, Nakajima M, Honda T, Kitao Y, Nakai O, Vreven H, Montgomery TJ, Peralta JA, Ogliaro JE, Bearpark F, Heyd M, Brothers JJ, Kudin E, Staroverov KN, Kobayashi VN, Normand R, Raghavachari J, Rendell K, Burant A, Iyengar JC, Tomasi SS, Cossi J, Rega M, Millam N, Klene JM, Knox M, Cross JE, Bakken JB, Adamo V, Jaramillo C, Gomperts J, Stratmann R, Yazyev RE, Austin O, Cammi AJ, Pomelli R, Ochterski C, Martin JW, Morokuma RL, Zakrzewski K, Voth VG, Salvador GA, Dannenberg P, Dapprich JJ, Daniels S, Farkas AD, Foresman Ö, Ortiz JB, Cioslowski JV, Fox J (2017) Gaussian 09, Revision E01. Gaussian Inc, Wallingford
23. Keith TA (2018) AIMAll http://aim.tkgristmill.com, Overland Park, 17.11.14 edn